# Four-phase merging in sessile compound drops

By L. MAHADEVAN†, M. ADDA-BEDIA and Y. POMEAU

Laboratoire de Physique Statistique de l'Ecole Normale Supérieure,
24 rue Lhomond, 75231 Paris Cedex 05, France

We consider the statics of compound droplets made of two immiscible fluids on a rigid substrate, in the limit when gravity is dominated by capillarity. In particular, we show that the merging of four phases along a single contact line is a persistent and robust phenomenon from a mechanical and thermodynamic perspective; it can and does occur for a range of interfacial energies and droplet volumes. We give an interpretation for this in the context of the macroscopic Young–Laplace law and its microscopic counterpart due to van der Waals, and show that the topological transitions that result can be of either a continuous or discontinuous type depending on the interfacial energies in question.

## 1. Introduction

Thermodynamics tells us that two bulk phases, like a liquid and its vapour at the same temperature, pressure and chemical potential(s), can coexist steadily along a two-dimensional surface. This is generic because two intersecting volumes in three-dimensional space meet along a surface. Three phases, like a liquid drop, its vapour and a flat solid, meet along a line that generically defines the intersection of a volume, its exterior and a plane. Thus one would expect four phases, for instance two immiscible liquids, a vapour and a solid, to merge at points, unless special conditions (on the mass of each liquid phase for instance) are satisfied. However, we show below that this may not be true: in some cases the merging of four phases at equilibrium occurs generically and persistently along a line (instead of at a point) and follows from a peculiarity of the Young–Laplace equilibrium conditions at the contact line.

When a small droplet of volume $V$ sits on a solid surface, its equilibrium shape is determined by the minimization of its capillary energy (in the formulation due to Gauss) associated with the interfacial area that it presents to its own vapour, subject to the constraint of a fixed volume, and appropriate boundary conditions at the triple line. In the absence of gravitational forces, the shape of the interface is simply a section of a spherical surface (in three-dimensions) and an arc of a circle (in two-dimensions). An equivalent treatment in terms of force balance requires that the droplet be axisymmetric (so that all torques are balanced), and that the interface and the triple line are determined by the Laplace law (Laplace 1806) relating the curvature of the interface to the difference in pressure between the liquid and its vapour, along with the Young–Laplace condition (Young 1805) at the triple line. The equilibrium equation for forces normal to the interface is

$$p_v - p_l \equiv \sigma_{lv}\kappa \qquad (1.1)$$

† Present address: Department of Applied Mathematics and Theoretical Physics, Silver Street, Cambridge CB3 9EW, UK
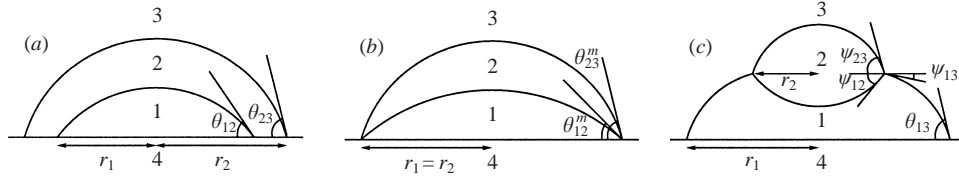
FIGURE 1. The different configurations of a composite drop of two immiscible liquids on a substrate. The numbers denote the phases: 1, liquid 1, 2, liquid 2, 3, vapour, 4, solid. (*a*) Configuration (I): liquid 2 encapsulates liquid 1 and there are two contact lines on the substrate. (*b*) Configuration (m): liquid 2 encapsulates liquid 1 and the contact lines merge. (*c*) Configuration (II): liquid 2 forms a drop that sits on liquid 1, and there are two contact lines, one on the substrate and one at the interface of the liquids.

where $\kappa$ is the mean curvature of the liquid–vapour interface and $p_v, p_l$ denote the pressure of the vapour and the liquid. The general solution to (1.1) is a surface of constant mean curvature, in this case simply part of the surface of a sphere (a spherical cap). Along the contact (triple) line, we must also balance forces; this leads to the well-known Young–Laplace condition

$$\sigma_{lv} \cos \theta = \sigma_{sv} - \sigma_{ls}. \tag{1.2}$$

Here $\sigma_{lv}, \sigma_{ls}, \sigma_{sv}$ denote the interfacial tension of the liquid–vapour, liquid–solid and solid–vapour interfaces respectively, and $\theta$ is the contact angle between the interface and the substrate. Together with the constraint of fixed volume, the above equations suffice to uniquely determine the shape of the drop and the pressure inside it in terms of the vapour pressure $p_v$ and the three interfacial tensions. A point that must be emphasized here is that the Young–Laplace condition only enforces force equilibrium in the plane of the solid; the vertical component of the liquid–vapour interfacial tension $\sigma_{lv} \sin \theta$ is unbalanced; of course there is no contradiction if the solid is assumed to be rigid. For a stiff solid such as glass, accounting for the vertical force leads to a deformation that is on the atomic scale, and therefore inconsequential, because of its very small contribution to the total energy. As we shall see, this degree of freedom will be crucial in determining a range of parameters over which four phases can merge robustly.

## 2. Macroscopic theory of four-phase merging

We now generalize the above picture, to consider the equilibrium shape of two immiscible fluids 1 and 2 adjoining a vapour 3 and sitting on a flat solid 4, that minimizes the capillary energy (this is actually the free energy in the case we are interested in) associated with the area of each interface bounding a bulk phase, subject to the usual volumetric constraints. In the present problem, there are *a priori* six capillary constants $\sigma_{ij}, i = 1 - 4, j = 1 - 4; \sigma_{ij} = \sigma_{ji}, (i \neq j)$ denoting the energy per unit area of the six possible interfaces separating the four phases.

Next, we consider the situation associated with a fixed volume $V_1$ of liquid 1, and a gradually varying volume $V_2$ of liquid 2. The configurations of the droplets must be axisymmetric to satisfy torque balance; however, there are three distinct states in which the drops can sit relative to each other, as shown schematically in figure 1(*a–c*), and denoted by configuration (I), (m) and (II) respectively. We will consider each one separately, but note that geometric continuity allows for a smooth transition from one

configuration to another. As we shall see for certain parameter ranges, considerations of force balance allow some of these states to persist for a range of drop volumes.

### 2.1. *Configuration (I)*

We consider configuration $(I)$ in figure 1($a$), a spherical cap of liquid 2 with a small droplet of 1 inside, the two fluid interfaces being disjoint. Let $R_{12}, R_{23}$ be the radii of the spherical caps that bound the interfaces 1–2 and 2–3 respectively. They are related to the contact radii of the drops $r_1$ and $r_2$ via the geometric relations

$$r_1 = R_{12} \sin \theta_{12}, \quad r_2 = R_{23} \sin \theta_{23}. \tag{2.1}$$

Then the volumes of the caps are given by

$$V_1 = \frac{\pi}{3} R_{12}^3 (2 - 3 \cos \theta_{12} + \cos^3 \theta_{12}), \quad V_2 + V_1 = \frac{\pi}{3} R_{23}^3 (2 - 3 \cos \theta_{23} + \cos^3 \theta_{23}). \tag{2.2}$$

The interfacial areas are given by

$$A_{12} = 2\pi(1 - \cos \theta_{12})R_{12}^2, \quad A_{23} = 2\pi(1 - \cos \theta_{23})R_{23}^2. \tag{2.3}$$

The equilibrium contact angles $\theta_{12}$, and $\theta_{23}$ for the drops of liquid 1, 2 sitting as shown in figure 1($a$) are determined by the Young–Laplace relations

$$\cos \theta_{12} = \frac{\sigma_{24} - \sigma_{14}}{\sigma_{12}}, \quad \cos \theta_{23} = \frac{\sigma_{34} - \sigma_{24}}{\sigma_{23}}. \tag{2.4}$$

Using the relations (2.1), (2.2) in the expressions for the drop volumes yields

$$\left(\frac{r_2}{r_1}\right)^3 = \left(1 + \frac{V_2}{V_1}\right) \frac{f(\theta_{23})}{f(\theta_{12})}, \tag{2.5}$$

where

$$f(\theta) \equiv \frac{1}{F(\theta)} \equiv \frac{\sin^3 \theta}{(2 - 3 \cos \theta + \cos^3 \theta)}, \tag{2.6}$$

and $f(\theta)$ is monotonically decreasing in the range $\theta \in [0, \pi]$. Furthermore the height of the 2–3 interface above the solid must be larger than that of the 1–2 interface, i.e. $R_{23}(1 - \cos \theta_{23}) > R_{12}(1 - \cos \theta_{12})$. By using (2.5) and (2.1) this inequality is

$$1 + \frac{V_2}{V_1} > \frac{f(\theta_{12})}{f(\theta_{23})} \left(\frac{\tan \frac{1}{2}\theta_{12}}{\tan \frac{1}{2}\theta_{23}}\right)^3. \tag{2.7}$$

For later use, we record the energy of configuration (I) which is

$$E_{(I)} = \sigma_{23} A_{23} + \sigma_{12} A_{12} + \pi R_{12}^2 \sin^2 \theta_{12}(\sigma_{14} - \sigma_{34})$$

$$+ \pi(R_{23}^2 \sin^2 \theta_{23} - R_{12}^2 \sin^2 \theta_{12})(\sigma_{24} - \sigma_{34}). \tag{2.8}$$

Here (and elsewhere) we have subtracted the infinite energy associated with the interaction of the solid plane and the vapour to obtain a finite result.

### 2.2. *Configuration (m)*

There are two possible routes to reach configuration $(m)$, shown in figure 1($b$), where four phases merge along the contact line on the solid. We may start from configuration $(I)$ with a large volume of liquid 2, i.e. $V_2 \gg V_1$ and reduce $V_2$ until the 2–3 interface meets the 1–2 interface. The other possibility is to start from configuration $(II)$ with an infinitesimal amount of liquid 2, i.e. $V_2 \ll V_1$, and gradually increase $V_2$.

Generically, these two ways of achieving configuration ($m$) will yield different values of $V_2/V_1$, since they represent limits of different topological configurations. Thus, we can expect that under certain conditions, the merger of four phases along a contact line can persist for a range of drop volumes, which we now proceed to show.

We first approach configuration ($m$) as a limiting case of configuration ($I$), when the two interfaces 1–2 and 2–3 merge along the solid. This corresponds to the intermediate configuration connecting figures 1($a$) and 1($b$). To determine the conditions when this state can exist, we substitute $r_1 = r_2 = r$ into condition (2.5), so that

$$1 + \left(\frac{V_2}{V_1}\right)^{(m)} = \frac{f(\theta_{12}^{(m)})}{f(\theta_{23}^{(m)})}. \tag{2.9}$$

In view of the inequality (2.7), we see that this requires that the equilibrium contact angles of the individual drops satisfy the inequality $\tan \theta_{12}/2 < \tan \theta_{23}/2$, i.e. $\theta_{12} < \theta_{23}$, for the merger of the contact lines to occur, consistent with the intuitive geometrical requirement evident in figure 1($b$). The Young–Laplace equation for the balance of horizontal forces in this configuration leads to

$$\sigma_{12} \cos \theta_{12}^{(m)} + \sigma_{23} \cos \theta_{23}^{(m)} = \sigma_{34} - \sigma_{14}. \tag{2.10}$$

$\theta_{12}^{(m)}$ and $\theta_{23}^{(m)}$ are still the angles between the solid and the surfaces of droplets 1 and 2, but they are not generally equal to their usual Young–Laplace values given in (2.4). However, for one particular value of the ratio $(V_2/V_1)^{(m)} = (V_2/V_1)^{(m')}$, (2.9) is satisfied with $\theta_{12}^{(m')} = \theta_{12}, \theta_{23}^{(m')} = \theta_{23}$, i.e. the contact angles have their equilibrium values given in (2.4). The critical value of the volume ratio when the contact lines merge is given by substituting this condition in (2.10) so that

$$1 + \left(\frac{V_2}{V_1}\right)^{(m')} = \frac{f(\theta_{12}^{(m')})}{f(\theta_{23}^{(m')})} = \frac{f(\theta_{12})}{f(\theta_{23})}. \tag{2.11}$$

When $V_2/V_1$ is different from $(V_2/V_1)^{(m')}$, conditions (2.10) and (2.9) determine $\theta_{12}^{(m)}, \theta_{23}^{(m)}$ as a function of the $V_2/V_1$, i.e. generically, we can expect a range of $V_2/V_1$ consistent with four-phase merging and energy minimization as embodied in (2.8). This one-parameter family of solutions is a direct result of the degree of freedom associated with not having to satisfy the balance of vertical forces along the four-phase contact line.

We can also approach configuration ($m$) as the limit of configuration ($II$) when the drop of liquid 2 rides on top of liquid 1 and just before it moves on to the solid substrate, the intermediate configuration connecting figures 1($b$) and 1($c$). By geometric continuity, the contact angle of drop 1 is associated with the equilibrium of the drop with vapour 3 (rather than with liquid 2), at this instant. Furthermore, the Young–Laplace condition (2.10) for the balance of horizontal forces must be supplemented by an additional equation for the balance of vertical forces, which then uniquely defines a second critical value of $(V_2/V_1)^{(m)} = (V_2/V_1)^{(m'')}$ that is consistent with the merger of the contact lines. In general $(V_2/V_1)^{(m')} \neq (V_2/V_1)^{(m'')}$, so that we can expect a range of values for $V_2/V_1$ where it is possible to have the robust merger of four phases.

### 2.3. *Configuration (II)*

So far, we have considered the configuration of the drops when both contact lines are on the solid, being disjoint or merged. Let us consider configuration ($II$) when drop 2 rides on drop 1, as shown in figure 1($c$). Here, although the interface 2–3 is spherical, the interface 1–3 is not necessarily so (and in general is just an axisymmetric surface

of constant mean curvature). However, a simple calculation shows that it is in fact spherical, greatly facilitating matters. The volumes of the two drops are given by

$$V_1 = \tfrac{1}{3}\pi r_1^3 F(\theta_{13}) - \tfrac{1}{3}\pi r_2^3 (F(\psi_{13}) - F(\psi_{12})), \quad V_2 = \tfrac{1}{3}\pi r_2^3 (F(\psi_{23}) - F(\psi_{12})), \quad (2.12)$$

where $F$ is defined in (2.6). The geometric identity $r_2/\sin\psi_{13} = r_1/\sin\theta_{13}$ leads to a relation analogous to (2.5) for the ratio of drop volumes given in (2.12) for configuration (II)

$$\left(\frac{r_2}{r_1}\right)^3 = \frac{\sin^3\psi_{13}}{\sin^3\theta_{13}} = \frac{(V_2/V_1)F(\theta_{13})}{(1 + V_2/V_1)(F(\psi_{13}) - F(\psi_{12})) + F(\psi_{23}) - F(\psi_{13})}. \quad (2.13)$$

Moving from geometric considerations to the balance of forces, along the contact line on the solid where the phases $1, 3, 4$ merge, horizontal equilibrium requires that

$$\sigma_{13}\cos\theta_{13} = \sigma_{34} - \sigma_{14} = \sigma_{12}\cos\theta_{12} + \sigma_{23}\cos\theta_{23}, \quad (2.14)$$

where the last equality follows from (2.4). Along the contact line where the liquid phases 1, 2, merge with the vapour 3, horizontal and vertical equilibrium demand the satisfaction of the Young–Laplace relations

$$\sigma_{13}\cos\psi_{13} = \sigma_{12}\cos\psi_{12} + \sigma_{23}\cos\psi_{23}, \quad \sigma_{13}\sin\psi_{13} = \sigma_{12}\sin\psi_{12} + \sigma_{23}\sin\psi_{23}. \quad (2.15)$$

As discussed in §2.2, for a critical volume ratio $V_2/V_1$ configuration (*II*) with one drop atop another smoothly approaches configuration (*m*) when the four phases merge along the contact line. Geometric continuity demands that for this special configuration denoted by $(.)^{(m'')}$

$$r_2 = r_1, \quad \psi_{13} = \theta_{13}, \quad \psi_{12} = \theta_{12}^{(m'')}, \quad \psi_{23} = \theta_{23}^{(m'')}. \quad (2.16)$$

Then, the Young–Laplace relations (2.15) are

$$\sigma_{13}\cos\theta_{13} = \sigma_{12}\cos\theta_{12}^{(m'')} + \sigma_{23}\cos\theta_{23}^{(m'')}, \quad \sigma_{13}\sin\theta_{13} = \sigma_{12}\sin\theta_{12}^{(m'')} + \sigma_{23}\sin\theta_{23}^{(m'')}. \quad (2.17)$$

Solving for the transition contact angles yields

$$\theta_{12}^{(m'')} = \theta_{13} + \cos^{-1}\frac{\sigma_{13}^2 + \sigma_{12}^2 - \sigma_{23}^2}{2\sigma_{12}\sigma_{13}}, \quad \theta_{23}^{(m'')} = \theta_{13} + \cos^{-1}\frac{\sigma_{13}^2 + \sigma_{23}^2 - \sigma_{12}^2}{2\sigma_{13}\sigma_{23}}, \quad (2.18)$$

and the critical volume ratio is obtained by substituting (2.16) into (2.13) so that

$$1 + \left(\frac{V_2}{V_1}\right)^{(m'')} = \frac{f(\theta_{12}^{(m'')})}{f(\theta_{23}^{(m'')})}. \quad (2.19)$$

For the persistent merger of four phases, $(V_2/V_1)^{(m')} > (V_2/V_1)^{(m'')}$; using (2.11) and (2.19) this yields

$$\frac{f(\theta_{12}^{(m')})}{f(\theta_{23}^{(m')})} > \frac{f(\theta_{12}^{(m'')})}{f(\theta_{23}^{(m'')})}. \quad (2.20)$$

For later use, we record the energy of the configuration (*II*) which is

$$E_{(II)} = 2\pi\sigma_{13}R_{13}^2(\cos\psi_{13} - \cos\theta_{13}) + 2\pi\sigma_{12}R_{12}^2(1 - \cos\psi_{12})$$
$$+ 2\pi\sigma_{23}R_{23}^2(1 - \cos\psi_{23}) + \pi R_{13}^2\sin^2\theta_{13}(\sigma_{14} - \sigma_{34}). \quad (2.21)$$
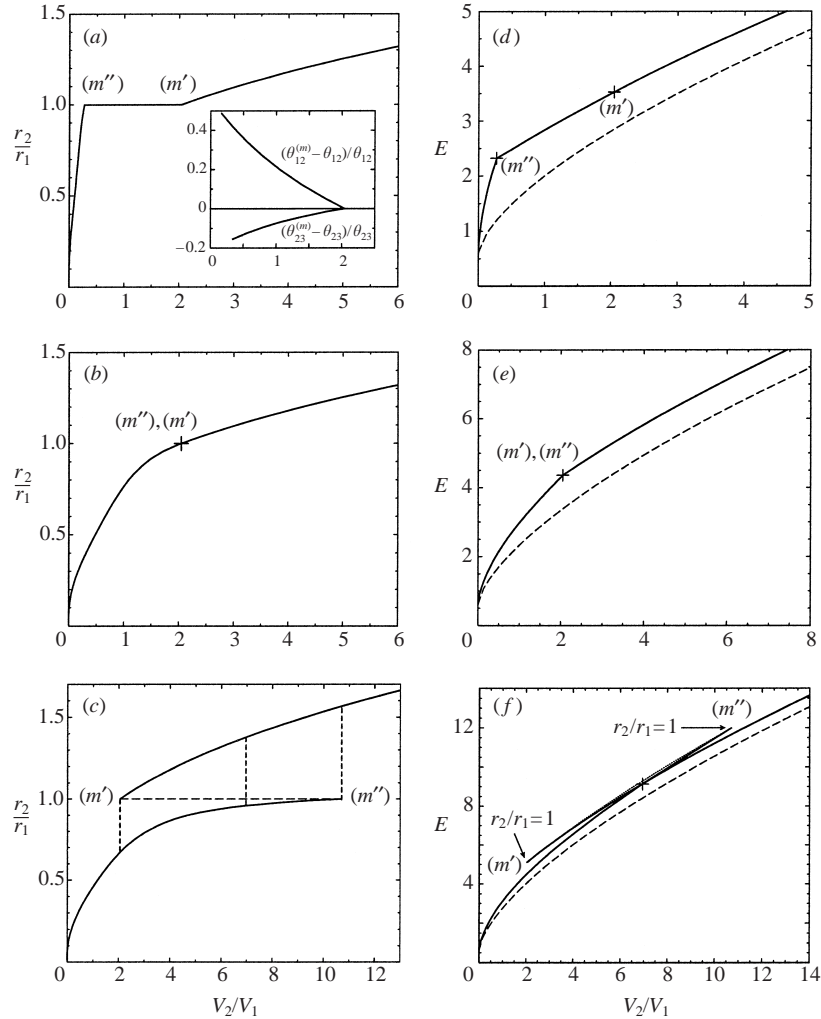
FIGURE 2. The ratio of the contact radii $r_2/r_1$ and the energy of the system $E$ as a function of the ratio of drop volumes $V_2/V_1$ for the configurations shown in figure 1, for different parameter values (given in the text) chosen so that $(a,d)$ $V_2/V_1^{(m')} > V_2/V_1^{(m'')}$, $(b,e)$ $V_2/V_1^{(m')} = V_2/V_1^{(m'')}$, $(c,f)$ $V_2/V_1^{(m')} < V_2/V_1^{(m'')}$. The dashed lines show the energy of disjoint drops on the substrate.

### 2.4. *Continuous and discontinuous transitions*

To illustrate the different cases, we choose some specific values for the equilibrium contact angles (interfacial energies) rather than choosing specific fluids. Since there are a total of six interfacial energies, and only energy differences are important, we can construct four dimensionless parameters, which can be some combination of the ratio of the interfacial energies and the equilibrium contact angles. To achieve the geometry shown in figure 1a, we must satisfy the inequality $\theta_{12} < \theta_{23}$; a particular choice is $\theta_{12} = \pi/4$, $\theta_{23} = \pi/2$. We also choose $\sigma_{12}/\sigma_{13} = 1$. This leaves one dimensionless parameter $\sigma_{23}/\sigma_{13}$ which we vary to show the different qualitative behaviours.

In figure 2, we show the variation in the ratio of the contact radii $r_2/r_1$ and the energy of the system $E$ as a function of the drop volume ratio $V_2/V_1$. Figure 2(a) corresponds to the case when $\sigma_{23}/\sigma_{13} = 1.1$ so that $(V_2/V_1)^{(m'')} < (V_2/V_1)^{(m')}$, leading

to persistent four-phase merger over a range of volume ratios. In the inset, we show the relative change in the contact angles $\theta_{23}^{(m)} - \theta_{23}/\theta_{23}$ and $\theta_{12}^{(m)} - \theta_{12}/\theta_{12}$ as a function of $(V_2/V_1)^{(m)}$ in the four-phase merger regime when $r_2/r_1 = 1$; interestingly, the variations are of the order of 30%. In figure 2(*d*), we show the variation in the energy of the system evaluated using (2.8); the energy varies continuously but suffers a jump in the slope at the critical volume ratios $(V_2/V_1)^{(m'')}$ and $(V_2/V_1)^{(m')}$. Figure 2(*b*) corresponds to the special case when $\sigma_{23} = \sqrt{2}\sigma_{13}$ so that $(V_2/V_1)^{(m'')} = (V_2/V_1)^{(m')}$, and phase merging occurs only for one value of $V_2/V_1$. The corresponding curve for the energy is shown in figure 2(*e*). Figure 2(*c*) corresponds to $\sigma_{23} = 1.7\sigma_{13}$ and so $(V_2/V_1)^{(m'')} > (V_2/V_1)^{(m')}$. The graph immediately suggests that the transition from configuration (*I*) to (*II*) is discontinuous in this case. This is clearly seen by considering the energy of the system computed using (2.8), (2.21) as shown in figure 2(*f*); the minimum energy solution corresponding to the line $r_2/r_1 = 1$ that connects the two critical volumes is larger than that associated with a path that corresponds to the dashed line in figure 2(*c*). Thus, we can generically expect a discontinuous transition from configuration (*I*) to (*II*) along the two dashed lines emanating at (*m'*) and (*m''*) depending on whether $V_2/V_1$ is being decreased or increased. In figure 2(*d–f*) we also plot the energy of two disjoint drops of liquid 1 and 2 on the substrate; in each case it is smaller than that of the composite drops, suggesting that composite drops are not global energetic minima. However, as we will argue later, they are local minima.

## 3. Towards a microscopic theory

Next, we complement the macroscopic considerations embodied in the macroscopic theory of the previous section by considering microscopic models of capillary phenomena. The classical example of such a theory is the so-called continuous-phase model or van der Waals model (van der Waals 1893). For simplicity, we will limit ourselves to two dimensions and only consider the limit where the interface slopes are small on microscopic scales, so that we can treat the liquid droplets as slender films. In this long-wavelength limit, the van der Waals model is closely related to the macroscopic Young–Laplace theory (Pismen & Pomeau 2000) making it possible to construct a consistent and uniform theory for static and dynamic contact lines.

We start by recalling the results for a single liquid/vapour interface merging with a solid. In two dimensions, the height of the interface $h = h(x)$ is a function of the horizontal coordinate $x$. The solid surface corresponds to the plane $z = 0$, the vapour phase is on the left when $x$ is large and negative and the liquid phase is on the right when $x$ is large and positive. The classical van der Waals theory leads to an equation for the equilibrium shape of the interface and can be formulated variationally. The functional that must be minimized to account for the interactions in the solid–liquid–vapour system may be written as

$$\mathscr{E}[h(x)] = \int_{-\infty}^{+\infty} \mathrm{d}x \left[ \frac{\sigma}{2} \left( \frac{\mathrm{d}h}{\mathrm{d}x} \right)^2 + U(h) \right]. \tag{3.1}$$

Here $\sigma$ is the surface tension of the liquid–vapour interface, the gradient term penalizes variations in the slope (or equivalently the density gradients in the classical van der Waals theory) and $U(h)$ is the interaction energy per unit length between the interface and the solid surface. The potential $U(h)$ has the following properties: $\partial U/\partial h|_{h^\star} = 0$, $U(h^\star) > 0$, $\lim_{h \to 0} U(h) = -\infty$, $\lim_{h \to \infty} U(h) = 0$.

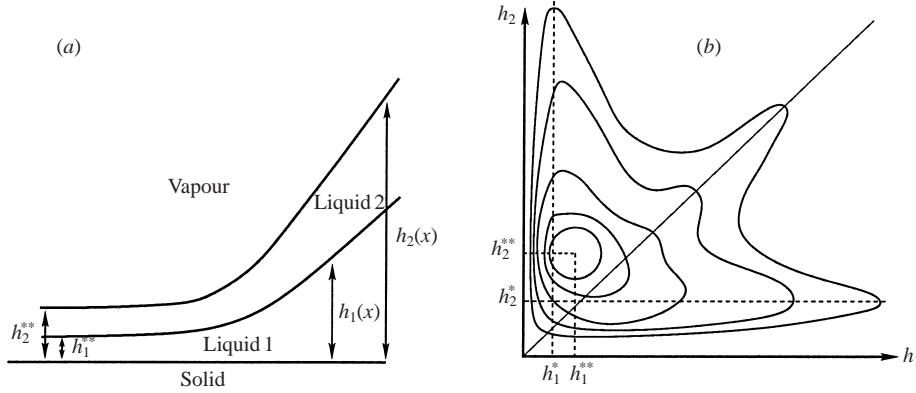The equilibrium merging of the interface with the solid is described by the solution

FIGURE 3. (*a*) A schematic of the four phases in the context of the microscopic van der Waals theory. $\sigma_1$ is the interfacial tension of the 1–2 interface, $\sigma_2$ that of the 2-vapour interface. (*b*) A schematic of the potential surface $U(h_1, h_2) = U_1(h_1) + U_2(h_2) + W(|h_1 - h_2|)$. The global equilibrium is denoted by $(h_1^{**}, h_2^{**})$.

of the Euler–Lagrange equation that arises from minimizing (3.1):

$$\sigma \frac{\mathrm{d}^2 h}{\mathrm{d}x^2} = \frac{\partial U(h)}{\partial h}, \qquad (3.2)$$

with the boundary conditions $\lim_{x \to -\infty} h = h^*$, and $\lim_{x \to +\infty} h \approx \theta x$, with $\theta \ll 1$ being the contact angle. Multiplying (3.2) by $\mathrm{d}h/\mathrm{d}x$ and integrating leads to an 'energy'-like integral of 'motion', which on using the boundary condition at infinity yields $\theta = \sqrt{U(h^*)/2\sigma}$. This is just the Young–Laplace condition for the present problem (Pismen & Pomeau 2000), and follows from the translational invariance of the functional (3.1).

We now extend the previous theory to the case of two different interfaces, one between liquid 1 and liquid 2 at height $h_1$, and another between liquid 2 and the vapour at height $h_2 > h_1$, as shown in figure 3. The generalization of the functional (3.1) to this case is

$$\mathscr{E}[h_1(x), h_2(x)] = \int_{-\infty}^{+\infty} \mathrm{d}x \left[ \sum_{i=1}^{2} \frac{\sigma_i}{2} \left( \frac{\mathrm{d}h_i}{\mathrm{d}x} \right)^2 + \sum_{i=1}^{2} U_i(h_i) + W(|h_1 - h_2|) \right]. \qquad (3.3)$$

Here $\sigma_1$ is the surface tension between liquid 1 and liquid 2, while $\sigma_2$ is the surface tension between liquid 2 and the vapour, the interaction potential between the fluid interfaces is $W(|h_1 - h_2|)$, while $U_1(h_1)$ and $U_2(h_2)$ represent the interaction potentials of the fluid interfaces with the solid substrate. The Euler–Lagrange equations that arise by minimizing (3.3) are

$$\sigma_1 \frac{\mathrm{d}^2 h_1}{\mathrm{d}x^2} = \frac{\partial U_1}{\partial h_1} + \frac{\partial W(|h_1 - h_2|)}{\partial h_1}, \quad \sigma_2 \frac{\mathrm{d}^2 h_2}{\mathrm{d}x^2} = \frac{\partial U_2}{\partial h_2} + \frac{\partial W(|h_1 - h_2|)}{\partial h_2}. \qquad (3.4a,b)$$

The general solution of (3.4) depends on four free parameters. One can be absorbed in the choice of the origin, since (3.4) forms an autonomous system in $x$, and two other conditions arise from the equilibrium heights of the interfaces far from the contact line $\lim_{x \to -\infty} h_1 = h_1^{**}, \lim_{x \to -\infty} h_2 = h_2^{**}$. This leaves one free parameter; for each asymptotic direction in the $(h_1, h_2)$ plane such that $h_1 < h_2$, a solution exists. As we shall see, this is the microscopic equivalent of the macroscopic Young–Laplace

condition that requires only a horizontal force balance for four-phase merging along a contact line.

There is more than one equilibrium solution corresponding to the vanishing of the right-hand sides of (3.4), which we now enumerate. In the case when phase 1 merges with the solid, we expect that $h_1 \gg h_2$, so that $W$ and $U_2$ are negligible. This corresponds to a local equilibrium where $\partial U/\partial h_1|_{h_1=h_1^*} = 0$; $U(h_1^*) > 0$. A similar scenario holds for the case when phase 2 merges with the solid, when $W$ and $U_1$ are negligible, and the local equilibrium is described by $dU/dh_2|_{h_2=h_2^*} = 0$; $U(h_2^*) > 0$. When the vapour merges with the solid, we expect that $h_1$ and $h_2$ have finite values, *a priori* unrelated to $h_1^*$ and $h_2^*$. Let $h_1^{**}$ and $h_2^{**}$ be the finite coordinates of this maximum of $U(h_1, h_2) = U_1(h_1) + U_2(h_2) + W(|h_1 - h_2|)$. The energy landscape $U(h_1, h_2)$ then has an isolated maximum at $h_1^{**}, h_2^{**}$, a ridge along or close to $h_1 = h_2$ for both $h_1$ and $h_2$ large, that describes $W$, the interfacial interaction term in $U$, and finally a ridge $h_1 = h_1^*$ when $h_2 \gg h_1$ that represents the liquid 2/solid interface. This is depicted schematically in figure 3.

The transition from the solid/vapour interface to the triple-phase merging is represented by a 'trajectory' leaving the fixed point $h_1^{**}$, $h_2^{**}$ at $x = -\infty$ to reach at $x = +\infty$ a trajectory such that $h_1 \approx \theta_1 x$ and $h_2 \approx \theta_2 x$. Multiplying (3.4*a*) by $dh_1/dx$, (3.4*b*) by $dh_2/dx$, adding the resulting equations and integrating the sum leads to

$$\sigma_1 \theta_1^2 + \sigma_2 \theta_2^2 = 2(U(h_1^{**}, h_2^{**}) - U(\infty, \infty)), \qquad (3.5)$$

leading to one equation between two unknowns, the angles $\theta_1 = dh_1/dx$ and $\theta_2 = dh_2/dx$. We have deliberately included the presence of the potential at infinity $U(\infty, \infty)$ to indicate its dependence on the limiting values of the two interfaces $h_1$ and $h_2$. The resulting one-parameter family of solutions in the microscopic theory mirrors the macroscopic freedom associated with the non-satisfaction of vertical force equilibrium in the Young–Laplace condition treated in §2.

The continuum of solutions may be indexed by the distance between $x_1$ and $x_2$, the locations where $d^2h_1(x_1)/dx^2$ and $d^2h_2(x)/dx^2$ are maximum. When this distance $|x_1 - x_2|$ is very large, one recovers two separate transitions, one from the vapour/solid interface to the liquid 2/solid interface, the other from the liquid 1/solid to the liquid 2/solid interface. In this case, the contact angles $\Theta_1$ and $\Theta_2$ are given by

$$\sigma_1 \Theta_1^2 = 2(U(h_1^{**}, h_2^{**}) - U(h_1^*, \infty)), \quad \sigma_2 \Theta_2^2 = 2(U(h_1^*, \infty) - U(\infty, \infty)), \qquad (3.6)$$

which are the Young–Laplace conditions for the contact angles in the usual three-phase merging situation. This corresponds to the case when the interaction potential $W$ vanishes so that one gets an additional 'integral of motion' associated with (3.4). In the general case, various limits associated with the relation of the interaction potential $W/U_i$ and the ratio of the interfacial tensions $\sigma_1/\sigma_2$ can exist, and may lead to interesting phase diagrams, which we will not treat here.

## 4. Discussion

In this paper, following a consideration of the equilibrium of compound drops made of two immiscible fluids on a rigid substrate we have shown that the merging of four fluid phases along a contact line can persist over a range of parameter values. The transition from one topological configuration to another for these drops can be either continuous or discontinuous depending on the relative interfacial energies (contact angles) of the various surfaces. While these effects can occur for entirely reasonable parameter values, the stability of these configurations remains an issue.

The robustness and stability of the four-phase contact line in configuration (m) is a given in the appropriate parameter regime. For small droplets (i.e. when the Bond number is small), gravitational effects are dominated by capillarity, and global balance of torques guarantees that stable compound drops remain axisymmetric to infinitesimal perturbations in configuration (II). In configuration (I), there is a weak translational invariance associated with the indeterminacy of the inner drop with respect to the outer one. However, as $V_2/V_1 \rightarrow 1$, this leads only to axisymmetric configurations which are stable. Stability of all these sessile configurations to finite perturbations is a much more difficult question (just as it is even for free drops); in fact two separate droplets can co-exist on the substrate and have a lower energy than the composite drop as depicted in figure 2(*d–f*). We will not address the issue further here.

We now briefly outline some implications of our study. The perceived hysteresis of the contact line of droplets in vapour environments of an immiscible liquid may be due to the effect treated here; small amounts of the immiscible fluid can coat the surface of the drop so that a range of contact angles becomes possible for small changes in the total drop volume. Thus it may be possible to use the persistent merger of contact lines in compound drops to change the effective capillary properties and thus circumvent the need for organic surfactants which are usually used fo this purpose, since the latter are stable only in a narrow temperature range. These ideas should also be applicable to bubbles on surfaces whose contact angles may vary appreciably due to a coating of an immiscible liquid. However, the main question that this study raises is the experimental feasibility of these configurations and transitions.

REFERENCES

LAPLACE, P. S. 1806 Sur l'action capillaire, *Suppl. au livre X, Traité de Mécanique Céleste*, p. 349.
PISMEN, L. & POMEAU, Y. 2000 Disjoining potential and spreading of thin films in the diffuse interface model coupled to hydrodynamics. *Phys. Rev.* E **62**, 2480.
VAN DER WAALS, W. 1893 The thermodynamic theory of capillarity under the hypothesis of a continuous variation of density. (English transl.). *J. Statist. Phys.* **20**, 197 (1979).
YOUNG, T. 1805 An essay on the cohesion of fluids *Phil. Trans. R. Soc.*, p. 65.